Journal of the Taiwan Institute of Chemical Engineers 000 (2021) 1–12

Contents lists available at ScienceDirect

Journal of the Taiwan Institute of Chemical Engineers

journal homepage: www.elsevier.com/locate/jtice

Direct surface modification of mesoporous silica nanoparticles by DBD plasma as a green approach to prepare dual-responsive drug delivery system

Sahar Porrang[a,b], Nader Rahemi[a,b,*], Soodabeh Davaran[c,d], Majid Mahdavi[e,f], Belal Hassanzadeh[g], Amin Mohammad Gholipour[h]

[a] Chemical Engineering Faculty, Sahand University of Technology, Sahand New Town, Tabriz, Iran
[b] Environmental Engineering Research Centre, Sahand University of Technology, Sahand New Town, Tabriz, Iran
[c] Department of Medical Nanotechnology, Faculty of Advanced Medical Science, Tabriz University of Medical Sciences, Tabriz, Iran
[d] Research Centre for Pharmaceutical Nanotechnology, Tabriz University of Medical Sciences, Tabriz, Iran
[e] Department of Biology, Faculty of Natural Science, University of Tabriz, Tabriz, Iran
[f] Department of Cell and Molecular Biology, Faculty of Biological Sciences, Kharazmi University, Tehran, Iran
[g] Faculty of Veterinary Medicine, University of Tabriz, Tabriz, Iran
[h] Department of Civil and Industrial Engineering, University of Pisa, Via Diotisalvi, Pisa, Italy

ARTICLE INFO

Article History:
Received 22 February 2021
Revised 6 May 2021
Accepted 13 May 2021
Available online xxx

Keywords:
Dielectric barrier discharge (DBD)
Direct surface modification
Dual-responsive
Drug delivery
Mesoporous silica nanoparticles
Rice husk

ABSTRACT

This paper deals with uniformly surface modification of mesoporous silica nanoparticles by applying dielectric barrier discharge (DBD) plasma as an energy-efficient and green approach. First, the mesoporous silica nanoparticles were synthesized from rice husk (RMSN-D) as an economic and biocompatible natural source. The surface modification stage by DBD plasma was performed in two methods: i) Direct mode and ii) Direct hybrid mode. The structure and physicochemical properties of the nanoparticles were characterized by XRD, FT-IR, Fe-SEM/EDS, TEM, EDS, BET, and H—NMR techniques. Doxorubicin (Dox) was exploited as a model drug, and in-vitro Dox release was investigated. The biocompatibility of nanocarriers was accepted by MTT test on HFF-2 cell line as a normal modal cell. For the advanced cellular study, apoptosis of the MCF-7 cell line treated with Dox-loaded nanocarriers was investigated by flow cytometric analysis and morphological study by fluorescent microscopy. The results showed that Dox-loaded RMSN-D modified by direct hybrid mode induced a high level of apoptosis in the MCF-7 cells.

1. Introduction

various modalities of cancer therapy such as the use of stimuli-responsive systems [1], active targeting approach, photothermal [2] and photo dynamic therapy [3] based on nanomaterials were fabricated. Due to mesoporous silica nanoparticle's (MSNs) unique properties such as: high surface area, high pore volume, stable mesopore structure, adjustable pore diameter/particle size, and simple internal and external surface functionalization [4-7], MSNs have several applications in various fields like bioimaging, photo-therapy, drug delivery, combination therapy [3, 8-14], adsorption of organic, inorganic, and gas compounds [15], catalyst [16, 17], enzyme immobilization [18], etc. Moreover, in drug delivery and cancer treatment fields, drug-loaded MSNs showed sustained release profile, which is the characteristic feature of the ideal drug delivery system [7, 19]. In the aim of drug delivery efficiency enhancement and design of a targetable drug delivery system, the MSNs surface could be functionalized by stimuli-responsive polymers. Poly (acrylic acid) as a pH-responsive polymer and poly(n-isopropylacrylamide) as a temperature-responsive polymer are Abundant used stimuli-responsive polymers that can be combined with MSNs to prepare an efficient drug delivery system to cancer treatment [20]. Free radical polymerization is the most frequently used method for obtaining various polymers and materials composites [21]. In this technique, free radicals play an essential role in initiating the polymerization process. Nowadays, the use of low-temperature atmospheric pressure dielectric barrier discharge (DBD) plasma systems for materials surface modification have gained considerable research interest [22-25]. In a plasma reactor, after applying a strong electric field at atmospheric pressure in the presence of reaction precursors, complex plasma species containing electrons, ions, neutral atoms, reactive species, metastable states, and UV radiation are created. These energetic species can transfer their momentum energy through direct collision with the material's surface and act as a reaction initiator at atmospheric pressure and moderate temperature [22-25]. Material's surface modification by plasma

* Corresponding author.
E-mail address: n_rahemi@sut.ac.ir (N. Rahemi).

https://doi.org/10.1016/j.jtice.2021.05.024
1876-1070/

technology as energy-efficient and green approach has advantages over the conventional chemical methods. Saving time and uniformly modification without affecting their physical and chemical bulk properties are some of these advantageous [26]. Moreover, The use of DBD plasma due to its simple structure and low cost as it does not require vacuum arrangements has become attractive in materials surface modification b plasma [25]. As mentioned before, plasma can be used to modify and even functionalize material surfaces. In 2012, Yan et al. used plasma technology to improve the surface of silica nanoparticles for increasing the interaction between surfaces to nanocomposite synthesis [27]. In a catalytic study, Rahmi et al. synthesized cold plasma-modified Ni−Cu/Al_2O_3 nanocatalysts [28]. The purpose of plasma in this study was to uniformly distribute the active phase of the catalyst on the base and increase the nanocatalyst activity. The use of plasma with the aim of mesoporous material templates has also been studied by researchers. For example, Yuan et al. in 2014, completely removed the P-123 template from the SBA-15 structure by oxygen plasma, which increased the specific surface area and silanol group density and caused CO_2 adsorption capacity enhancement [29]. Some researchers have directly modified the surface of the material with plasma technology to create the desired functional groups at the material's surface. Roucoules et al. succeeded in the porous surface of polystyrene functionalization with amine group by use of allylamine monomer vapor as a plasma reactor feed. Compared to chemical modification, this method was inexpensive, solvent-free, and the products were synthesized with smaller particle size and a higher density of amine group [30]. Taraballi et al. also enriched amine and carboxylic functional groups on collagen using N_2/H_2 and CO_2 plasma as widely used materials in tissue engineering [26]. From the point of view of plasma technology applications in medicine, we can mention the use of this technology in the sterilization of implants and surgical instruments as well as the modification of the surface of implants [31] to increase biocompatibility. In comparison, scientists have conducted studies in the field of skin diseases treatment [32] and cancer [33] with the help of this technology. So far, no extensive studies have been conducted in terms of using this technology in drug delivery and manufacturing of drug nanocarriers.

Herein, we propose a facile, economic, biocompatible, and efficient strategy for synthesis dual pH and thermo-responsive biogenic mesoporous silica nanoparticles, which were extracted from rice husk. High biocompatibility, good dispersity, uniformly surface modification, and higher toxicity compared with free Dox at the cancerous sites are fantastic features of the synthesized drug delivery system. Doxorubicin (Dox) has been chosen as a model chemotherapeutic agent, and HFF-2 and MCF-7 cell lines were chosen as normal and cancerous model cells, respectively. The cytotoxicity of the RMSN-D, RMSN-DPAN, and RMSN-DHPAN onto the HFF-2, and MCF-7 cell lines were measured. Also, the drug release behavior of the nanocarriers in the cancerous and normal sites was investigated. Moreover, apoptosis, as the mechanism of cell death, was evaluated by a morphological study of cells and flow cytometric analysis.

2. Experimental

2.1. Materials

Rice husk was prepared from a rice mill in Iran as a precursor for synthesizing silica nanoparticles. Hydrochloric acid to rice husk purification, sulfuric acid to regulate acidity, Cetyl trimethyl ammonium bromide (CTAB: 99%) as a surfactant, sodium dodecyl sulfate (SDS) as a structure-directing agent, ammonia solution 25% as a catalyzer, and Dimethyl sulfoxide (DMSO) were purchased from Merck (Darmstadt, Germany). Triethoxyvinylsilane (TEVS: 97%) as silane coupling agent, acrylic acid (AA), n-isopropylacrylamide 97% (NIPAAm: 97%), and potassium persulfate were purchased from Sigma-Aldrich, Chemical Co (St. Louis, MO USA). The RPMI-1640 as a cell culture medium, fetal bovine serum (FBS), and penicillin-streptomycin were procurement from Gibco (Life Technologies, Paisley, Scotland). HFF-2 and MCF-7 cell lines were obtained from the Pasteur Institute of Iran (Tehran, Iran). The 5-diphenyl-2-H-tetrazolium bromide (MTT), Trypsin, Hoechst 33,342, and Propidium Iodide powder were bought from Sigma-Aldrich, Chemical Co (St. Louis, MO USA). Doxorubicin hydrochloride (Dox) as a model drug was bought from the Faculty of Tabriz Pharmaceuticals, Iran.

2.2. DBD plasma set up

The system in this study consists of four main parts, including a high voltage power supply, DC generator, DBD batch plasma reactor, and control board, which are illustrated in Scheme 1. The power supply is responsible for supplying the energy required by the plasma to generate the discharge, which provides a variable voltage of 0−50 V with a maximum current of 5 A. A high voltage convertor regulated the voltage and frequency with a maximum value of 30 kV and 1 mA. The plasma reactor has consisted of two electrodes and a quartz dielectric barrier to generate non-thermal plasma with 1.5 mm thickness and 25 cm height. The reaction precursors as a reactor feed were placed in the inner chamber of the dielectric barrier. A steel rod is placed in direct contact with the reaction mixture as an internal cathode electrode connected to high voltage current. The copper outer electrode as an anode winding was placed in the form of a coil around the dielectric barrier. A magnet stirrer for preventing the precipitation of nanoparticles in solution was placed under the plasma reactor. The control board equipped with a fuse was intended for safety.

2.3. Synthesis method

2.3.1. RMSN-D synthesis

Rice husk, after washing with water and treated by 1 M hydrochloric acid for 3 h at 90 °C, and then drying, was calcined at 550 °C for 4 h at a rate of 5 °C/min. The product was the silica nanoparticle was named RSN. 1 g of RSN was dissolved in 7.04 mL of 1 M sodium hydroxide solution at 80 °C to prepare sodium silicate solution. The surfactant solution was prepared by dissolving 8 g of CTAB in 100 mL of deionized water at 40 °C, and the acidity of the solution was adjusted to 6.5 by 1 M sulfuric acid. Then sodium silicate solution was added to the surfactant, and at the end, the pH of the mixture was adjusted to 11.25 with 1 M NaOH solution and the mixture was stirred for 1 hour. The reaction mixture was kept at 100 °C for 24 h, and finally, the product at the bottom of the vessel was washed several times with a vacuum filter by distilled water. The sample was then calcined at 500 °C for 4 h at a rate of 5 °C/min. Similarly, mesoporous silica nanoparticles named RMSN-D were synthesized [7].

2.3.2. Direct surface modification by DBD plasma

The TEVS as a silane coupling agent was used to create the vinyl group on the RMSN-D nanoparticles. The surface modification stage by DBD plasma was performed in two methods. i) Direct mode: RMSN-D nanoparticles were modified by the vinyl group in the DBD plasma reactor tank (RMSN-DPV), and then, Acrylic acid (AA), and N-isoptopylacrylaminde (NIPAAm) monomers were polymerized in N_2 atmosphere on the surface of the modified nanoparticle (RMSN-DPAN). Briefly, 0.1 g RMSN-D and 1.76 mL TEVS were added into the 26.6 mL ethanol, 6.6 mL deionized water, and 40 μL ammonia solution 25%, followed by ultrasonic treatment for 15 min. Then the mixture was transferred to the DBD plasma reactor tank, and the system had run for 30 min with a voltage and a current value of 20 kV and 0.98 mA, and vigorously stirring. At the end of the process, vinyl modified RMSN-D named RMSN-DPV was centrifuged at 9000 rpm for 10 min and dried at 40 °C during the night. Afterward, 100 mg RMSN-DPV, 732 mg NIPAM, 270 μl AA, and 21.2 mg SDS were dissolved in 90 mL deionized water under an N_2 atmosphere at 70 °C for

Please cite this article as: S. Porrang et al., Direct surface modification of mesoporous silica nanoparticles by DBD plasma as a green approach to prepare dual-responsive drug delivery system, Journal of the Taiwan Institute of Chemical Engineers (2021), https://doi.org/10.1016/j.jtice.2021.05.024

1 h. Then, the KPS solution (54 mg in 5 mL deionized water) was added drop by drop in the mixture, and the reaction was accomplished at 70 °C for 6 h. The products were dialyzed (MWCO: 12,000 Da) against deionized water for 3 days, and then lyophilized. ii) Direct hybrid mode: Initially, the 100 mg RMSN-D nanoparticles were dispersed in 20 mL deionized water, and the mixture was transferred in the DBD plasma tank and treated with this system for 30 min with a voltage and a current value of 20 kV and 0.98 mA, and vigorously stirring. Then the pretreated RMSN-D was modified by the vinyl group in the presence of DBD-plasma (RMSN-DHPV), and stimuli-responsive polymers were created on its surface in an N_2 atmosphere (RMSN-DHPAN) as described in the direct mode section.

2.4. Phase transition and swelling behavior of RMSN-DPAN and RMSN-DHPAN

To evaluate the phase transition point of RMSN-DAN, 30 mg of nanoparticle was entirely dissolved in 1 ml PBS with pH equal to 5.4 at 4 °C to obtain a transparent solution of RMSN-DAN. Then the mixture temperature gradually increased. The lower critical solution temperature (LCST) was determined as the temperature when a swelling–deswelling transition suddenly occurred. Therefore, the temperature at which the solution becomes opaque was considered as the LCST point [1]. To swelling investigation, normal and cancerous site conditions were considered. 0.3 g of RMSN-DAN was immersed in 20 mL of PBS with various solutions at the given pH and temperature for 2 days [1].

The swelling ratio (gram per gram) of the nanoparticle was calculated according to the following equation:

$$\text{Swelling ratio}\ (\%) = (W_t - W_d) * 100/W_d \quad (1)$$

W_t: swollen weight and W_d: dried weight.

2.5. Drug loading into the nanocarriers

The Dox loaded nanocarriers were prepared by adding 4.5 mg Dox solution (2 mg/mL) to the nanocarriers solution (30 mg of nanocarriers in 3 ml deionized water). The mixture was stirred for 24 h in the darkroom. The mixture was centrifuged at 9000 rpm for 4 min and washed with distilled water twice. The amount of loaded drug into the nanocarriers was calculated using a UV spectrophotometer with a detection wavelength of 482 nm.

2.6. In vitro drug release behavior

The release of Dox in-vitro was investigated by dispersion of Dox loaded nanocarriers in 4 mL of PBS with two different pH values of 7.4, and 5.4. The dispersions were shaken transferred at the desired temperature in the shaker incubator. For consecutive times, the dispersions were centrifuged, and the supernatant was replaced by fresh PBS. The amount of released drug was determined using a UV spectrophotometer with the detection wavelength of 482 nm.

2.7. Cell culture

In this study, human breast cancer cells (MCF-7 cell line) and Human foreskin fibroblasts cells (HFF-2 cell line) were chosen as model cancerous and normal cells for toxicity investigation. The cells were cultured in RPMI 1640 medium supplemented with 10% (v/v) fetal bovine serum (FBS) and penicillin (100 U/ml). They were stored in an incubator at 37 °C in 5% CO2 humidified atmosphere [20].

2.8. The cytotoxicity assay

The toxicity of nanocarriers was investigated in three stages. i) MTT test of blank nanocarriers on HFF-2 cell line with the nanocarriers concentrations ranging from 0.4 to 200 $mg.ml^{-1}$. ii) MTT test of Dox loaded nanocarriers on MCF-7 cell line with the Dox concentrations ranging from 0.08 to 20 $mg.ml^{-1}$. iii) MTT test of blank nanocarriers on MCF-7 cell line with the same Dox concentrations. Briefly, the HFF-2 and MCF-7 cells were seeded onto 96-well plates (10^4 cell/well) and incubated for 24 h. Then the cells were treated with samples was described above. After 48 h, 20 μL of the MTT solution (5 mg/mL in PBS) was replaced in each well and incubated for an additional 3 h. Eventually, the absorbance of wells was recorded at 570 nm with a multi-well plate reader. Untreated cells in the medium were used as a control. All experiments were carried out with three replicates [1, 20].

2.9. Morphological evaluation of the apoptotic cells

For the morphological studies of the untreated and treated MCF-7 cell line with free Dox, and Dox loaded nanocarriers, the cells were seeded in 6-well plates at a concentration of 8×10^5 cells/well, in 2 ml of the growth medium, and incubated for 24 h to allow cell attachment. After that, the cells were treated with samples in IC50 values obtained by the MTT assay. After 48 h of incubation, The DNA was also stained with Hoechst 33,258 (1 mg/mL in PBS) for 2 min, then examined using a fluorescence microscope [1, 34].

2.10. Cell cycle analysis

The cell cycle studies Were performed to investigate the effect of the untreated and treated MCF-7 cell line with free Dox and Dox loaded nanocarriers. The treating procedure was the same as morphological evaluating. After 48 h incubation, the contents of the wells were transferred to the microtubes and washed twice by PBS. Then the cells were fixed in 600 μl ethanol (70%) and stored at 4 °C for 3 days. Then, each microtube's supernatant, which was obtained by centrifuge, was discarded, and was replaced with 100 μL Propidium iodide (PI) solution (20 μL/mL PBS). In the end, the cells were analyzed by flow cytometry [1, 35].

3. Characterization

The low angle and normal X-ray diffractometer (XRD) patterns of nanoparticles were recorded using a powder X-ray diffractometer (D8 Advance, Bruker AXS, Germany) with the scattering angle (2θ) range of 10–80° for the RSN, and 1 – 10° for RMSN-D. Fourier transform infrared (FT-IR) spectra were recorded using the FT-IR spectrophotometer (TENSOR 27, Bruker, Germany). The nanoparticles were visualized by Scanning electron microscopy (SEM) (TESCAN Vega 3, Kohoutovice, Czech Republic) and TEM (Bruker, Germany). Moreover, the energy-dispersive X-ray spectrum (EDS) were taken. N2 adsorption-desorption isotherms and parameters such as surface area, pore size, and pore volume were obtained with Surface Area and Pore Size Distribution Analyzer (Belsorp mini, japan).

4. Results and discussion

4.1. Characterization

The overall procedure used to synthesize the RMSN-D from rice husk and its modification process by DBD plasma with i) direct and ii) direct hybrid modes are illustrated in Scheme 2. Details of the steps taken to synthesize mesoporous silica nanoparticles from rice bran and the reactions performed in the DBD plasma reactor to modify the nanoparticle's surface as well as the polymerization of AA and NIPAAm monomers on the modified nanoparticle surface are also shown in Scheme 2.

Please cite this article as: S. Porrang et al., Direct surface modification of mesoporous silica nanoparticles by DBD plasma as a green approach to prepare dual-responsive drug delivery system, Journal of the Taiwan Institute of Chemical Engineers (2021), https://doi.org/10.1016/j.jtice.2021.05.024

4.2. Scheme 2

Biogenic silica nanoparticle (RSN) as a precursor to RMSN-D synthesis, was extracted from rice husk. Fig. 1 illustrated the wide-angle XRD pattern of RSN and the low-angle XRD pattern of RMSN-D. As illustrated in Fig. 1-a, RSN was amorphous in nature and had a characteristic broad peak at a 2θ angle of 22.17°, indicated the amorphous nature of silica. Also, no impurities were observed in the profile. Fig. 1-b shows the low-angle XRD pattern of RMSN-D. The XRD pattern showed the crystalline state of silica with an intense peak at a 2θ = 2.36° related to the reflection line (100), which characteristic of the hexagonal structure of the mesoporous silica nanoparticles with high crystallinity [1, 7, 36].

To obtain an infrared spectrum of nanocarriers to investigate the chemical groups on them, the FT-IR analysis was performed at the same condition for all the nanoparticles. As illustrated in Fig. 2, The characteristic bands of silica nanoparticles were visible at 460 cm^{-1}, 810 cm^{-1}, and 1100 cm^{-1} due to the asymmetric and symmetric stretching of Si–O–Si in all samples. The peak at 3450 cm^{-1} was related to symmetric stretching of the Si-OH group [1, 7]. By plasma modification of RMSN-D surface to inducing vinyl group, as illustrated in Fig. 2-c and d, the intensity of the surface silanol group decreased significantly. Moreover, the band at 2975 cm^{-1} was associated with the C—H of vinyl groups. So, the vinyl group was successfully created on the RMSN-D surface by the plasma technique. Also, the C = C group of TEVS was overlapped with the O—H stretching vibration of H_2O at 1620 cm^{-1}. After creating the vinyl group on the nanoparticles surface, the stimuli-responsive polymers were formed on the modified nanoparticles by the radical polymerization method. As showed in Fig. 2-e and f, the NIPAAm N–H stretching band was visible at 1542 cm^{-1}, and C–N stretching signals at 1455 cm^{-1}, and 1385 cm^{-1} have appeared from the amide group in NIPAAm. Peaks at 1725 cm^{-1}, and 1542 cm^{-1} were related to C = O, and the signal at 1639 cm^{-1} was related to C = O, and C = C groups, respectively. The peaks at 2973 cm^{-1}, and 1254 cm^{-1} were related to C–H band from the isopropyl group in NIPAAm [1]. The results of FT-IR analysis indicated the correct synthesis of functionalized mesoporous silica nanoparticles with temperature and pH-sensitive polymers by the plasma technique.

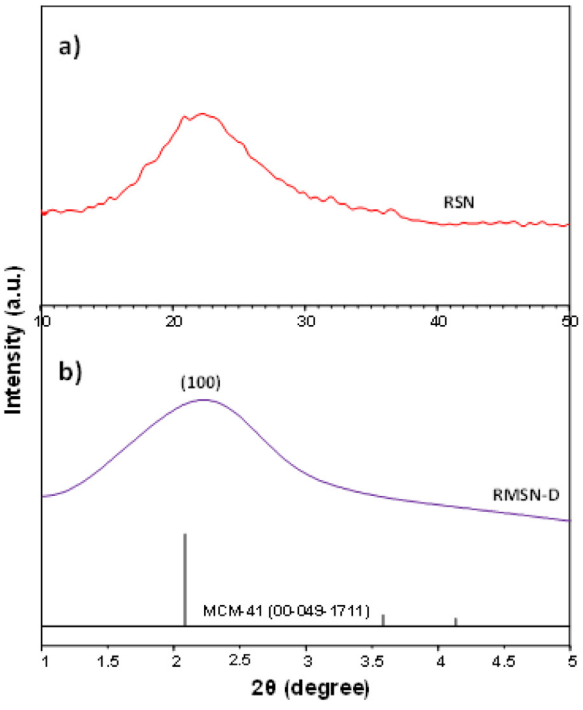

Fig. 1. X-Ray diffraction patterns of the silica nanoparticles: (a)RSN and (b) RMSN-D.

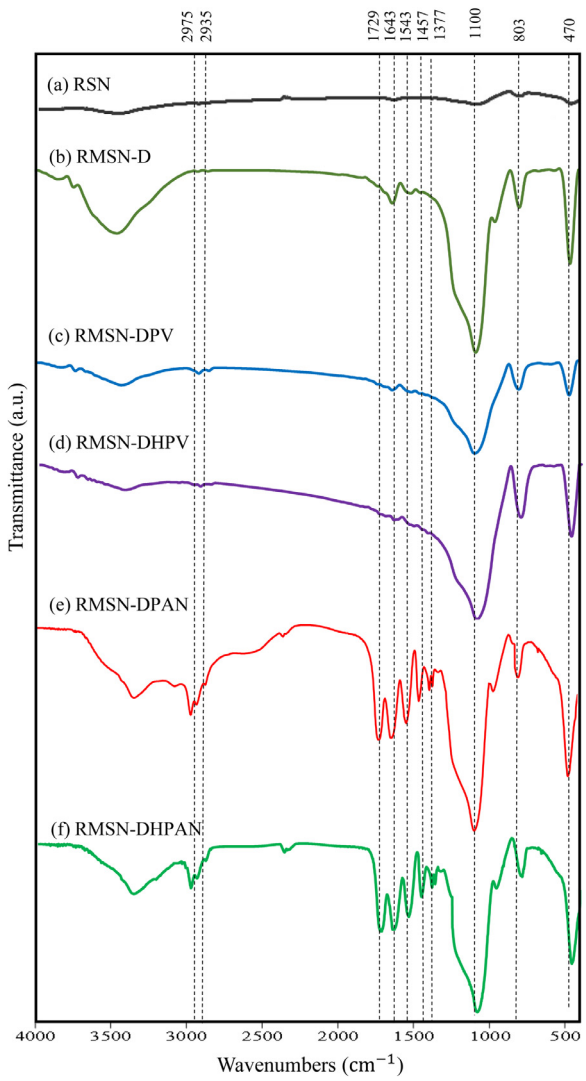

Fig. 2. FT-IR spectra of (a) RSN (b) RMSN-D (c) RMSN-DPV (d) RMSN-DHPV (e) RMSN-DPAN and (f) RMSN-DHPAN.

The surface morphology and structural properties of nanocarriers were analyzed by the Field emission scanning electron microscope (FE-SEM) and Transmission electron microscope (TEM). Fig. 3 represented the Fe-SEM and TEM images of (a)RMSN-D, (b)RMSN-DPAN, and (c) RMSN-DHPAN. Fe-SEM result for nanocarriers revealed a uniform, discrete spherical shape with a particle size of about (a)42, (b) 102, and (c)162 nm, respectively. The TEM image of RMSN-DPAN, and RMSN-DHPAN showed were more uniform and separated from one another. However, the presence of Si, O elements for RMSN-D and the presence of Si, O, C, and N elements for RMSN-DPAN, and RMSN-DHPAN were confirmed by Energy-dispersive X-ray spectroscopy (EDS). The percentage of elements was reported in Table 1.

The specific surface area, specific pore volume, and the average pore volume are characteristic parameters that influence the drug delivery capacity of nanocarriers. To investigate these parameters, the BET analysis was performed. Fig. 4-a illustrated the N2 adsorption/desorption isotherms of RSN, RMSN-D, RMSN-DPV, RMSN-DHPV, RMSN-DPAN, and RMSN-DHPAN. According to IUPAC classification, the RSN and RMSN-D isotherms represent type IV,

Please cite this article as: S. Porrang et al., Direct surface modification of mesoporous silica nanoparticles by DBD plasma as a green approach to prepare dual-responsive drug delivery system, Journal of the Taiwan Institute of Chemical Engineers (2021), https://doi.org/10.1016/j.jtice.2021.05.024

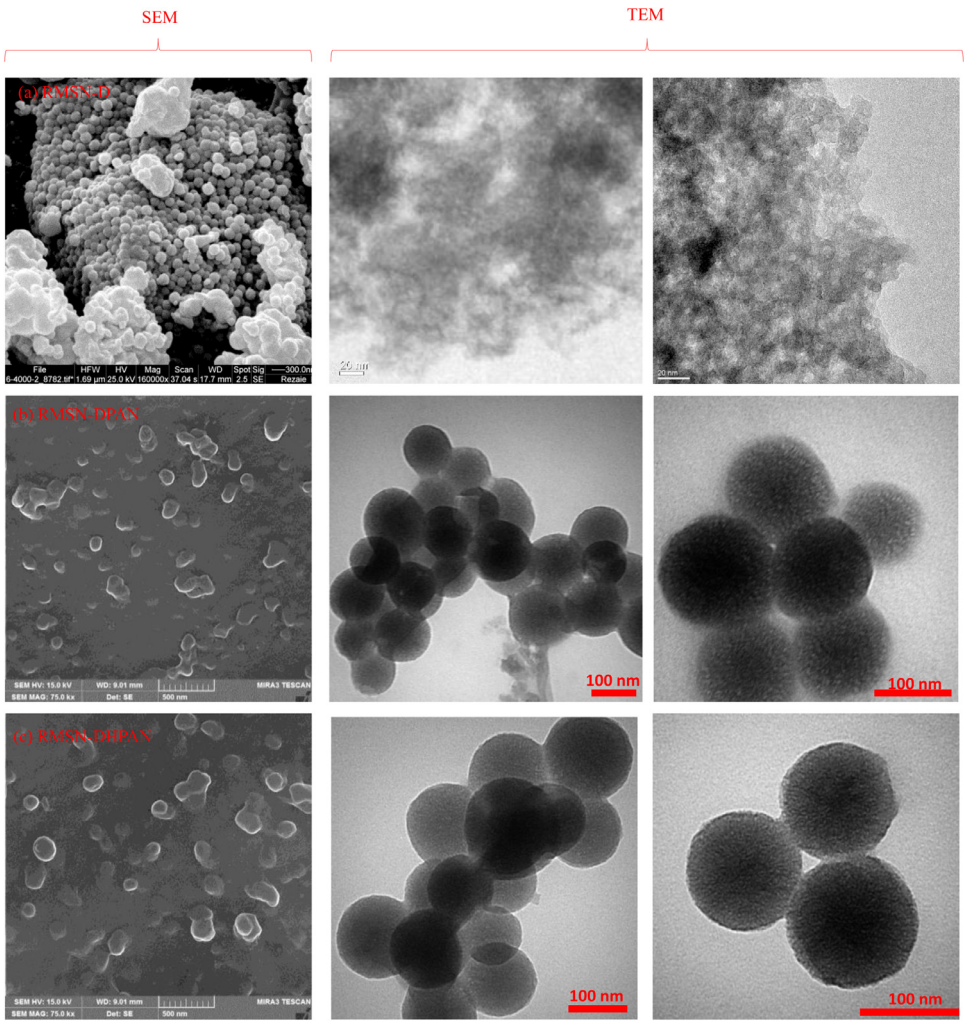

Fig. 3. FE-SEM and TEM images of (a) RMSN-D (b) RMSN-DPAN, and (c) RMSN-DHPAN.

Table 1
mass percentage of elements in nanoparticles.

Elements (W%)	RMSN-D	RMSN-DPAN	RMSN-DHPAN
Si	71.02	12.90	12.94
O	28.98	29.68	35.19
C	–	50.25	47.03
N	–	7.29	4.84

which confirmed the existence of a mesoporous structure [1, 7]. Also, after surface functionalization by direct and direct hybrid plasma approach, the RMSN-DPV and RMSN-DHPV had porous structure and the N2 adsorption/desorption data represent type IV isotherm. RSN, RMSN-D, RMSN-DPV, and RMSN-DHPV had a specific surface area of 226.52, 950.76, 703.58, and 690.75 cm^2g^{-1}, respectively. Also, the average pore volume of them was 0.2498, 1.1218, 0.8756, and 0.7659 cm^3g^{-1}. The lower specific surface area and specific pore volume of vinyl modified nanoparticles compared to RMSN-D indicates the success of the surface modification step. Fig. 4-b showed the pore size distribution of nanoparticles. The RSN, RMSN-D, RMSN-DPV, and RMSN-DHPV had a narrow pore size, and the BJH peak pore diameter of them was 3.32, 2.44, 2.43, and 2.42 nm, respectively. Furthermore, the surface area, pore volume, and pore diameter of RMSN-DPAN and RMSN-DHPAN cannot be calculated, because the RMSN-D completely be trapped in the polymeric shell [1]. So, as illustrated in Fig. 4, the N2 adsorption-desorption parameters of RMSN-DAN cannot be detected.

Fig. 5-a and b show the ^{1}H NMR spectra of RMSN-DPAN, and RMSN-DHPAN in DMSO. The characteristic proton signal at 1.03 ppm assigned to $(CH_3)_2CH-$, and the signal at 3.8 ppm belonged to $(CH_3)_2CH-$ (isopropyl group) in NIPAAm [37-39]. However, the signal attributed to $-CH_2-$ of NIPAAm and AA appeared at 1.5 and 2 ppm [1, 40]. The signal at 7.2 ppm related to NH of NIPAAm, and the signal at 12.1 ppm assigned to OH of AA [1, 40]. The ^{1}H NMR spectrum confirmed that the AA and NIPAAm were polymerized successfully on the RMSN-D surface.

The LCST point of RMSN-DPAN and RMSN-DHPAN was determined by detecting the phase transition of nanocarriers solution in the PBS with pH 5.4. By increasing the temperature to 38 °C, the solutions become opaque from the transparent state. So, 38 °C was considered as the LCST point of nanocarriers, which is an essential parameter in drug release behavior. The swelling percentage of nanocarriers was investigated at the body (37 °C and pH=7.4) and cancerous site (40 °C and pH=5.4) conditions for 48 h. The swelling percentage of RMSN-DPAN and RMSN-DHPAN at the body condition was 241 and 289%. This parameter for nanocarriers at cancerous site was 73 and 49%. So, the nanocarriers especially RMSN-DHPAN have a more significant swelling percentage at normal tissues in the body, which act as smart gatekeepers and protect drugs from premature release. However, in cancerous site conditions, nanocarriers were in

Please cite this article as: S. Porrang et al., Direct surface modification of mesoporous silica nanoparticles by DBD plasma as a green approach to prepare dual-responsive drug delivery system, Journal of the Taiwan Institute of Chemical Engineers (2021), https://doi.org/10.1016/j.jtice.2021.05.024

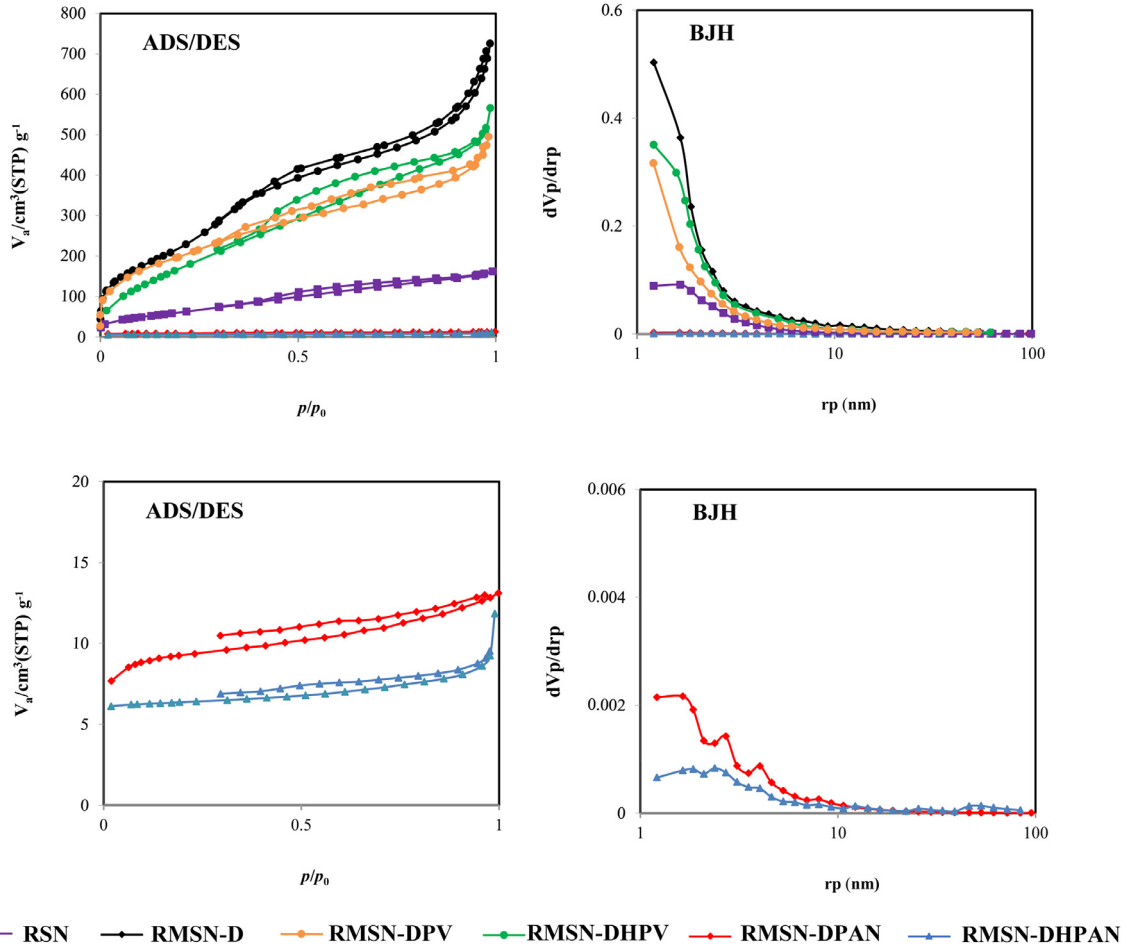

Fig. 4. The (a) N2 adsorption–desorption isotherm and (b) BJH pore diameter distribution of RSN, RMSN-D, RMSN-DPAN and RMSN-DHPAN.

collapse form, and the polymeric shell allows chemotherapeutic to release.

4.3. In-vitro drug release behavior

To in-vitro drug release investigation, Dox as a model anti-cancer drug was loaded into RMSN-D, RMSN-DPAN, and RMSN-DHPAN with a drug loading percentage of 35, 56, 42%, respectively. RMSN-DPAN and RMSN-DHPAN had higher Dox loading percentage compared to RMSN-D due to polymeric cover around nanoparticles, which the drug molecules could be trapped into the polymeric shell. Moreover, because of the smaller size of RMSN-DPAN compared to RMSN-DHPAN, it had a higher Dox loading percentage. Since extracellular acidity, especially intracellular acidity, is lower in cancerous tissues [1, 7, 39, 41, 42] and the temperature in these areas is slightly higher (40 °C) [1, 7, 39] than normal tissues and blood flow, in this study, drug release behavior was investigated in the following three conditions: i) T = 37 °C, and pH= 7.4 (physiological condition), ii) T = 37 °C, and pH= 5.4 (To investigate the pH effect in constant temperature, and iii) T = 40 °C, and pH= 5.4 (cancerous site condition, and the temperature effect can investigate against condition ii). As shown in Fig. 6-a, the cumulative Dox release from RMSN-D and RMSN-DPAN was investigated at the above conditions. 29.6% of loaded Dox in RMSN-D released at condition (i); However, 46.6%, and 49.8% of loaded Dox can release at conditions (ii) and (iii) for 96 h, respectively. The higher Dox release amount at a lower pH value was due to Dox's higher solubility in this condition. A lower pH cause Dox amine group protonation raising. So, the hydrophilicity of Dox is enhanced [43]. As the temperature rises to 40 °C, no significant change was observed in the amount of drug released between conditions (ii) and (iii). However, by employing the pH and temperature-responsive RMSN-DPAN, the amount of released Dox at condition (i) reduced to 18%. However, at cancerous condition (iii), the amount of released Dox enhanced to 82.2% for 96 h. As shown in Fig. 6-a, by keeping the temperature constant at 37 °C and reducing the pH to 5.4, the final amount of drug released for 96 h is 65.3%, which indicates the effect of acidity on increasing drug release. By comparing conditions (ii) and (iii) in Fig. 6-a, the positive effect of rising temperature at constant pH on increasing the amount of drug release can be seen. Fig. 6-b also compared the Dox release amount from RMSN-D and RMSN-DHPAN samples in three various conditions for 96 h. The released Dox percentage from RMSN-DHPAN in conditions (i), (ii), and (iii) was 12.6%, 73.4%, and 98%, respectively. However, this system showed better pH and temperature responsive behavior. Fig. 6-c illustrated a comparative Dox release percentage from RMSN-DPAN and RMSN-DHPAN nanocarriers. In condition (i), Dox-loaded RMSN-DHPAN releases 5.5% lower drug into the normal body site simulator medium which can minimize the side effect of Dox. It has also been able to release 15.8% more drugs in simulated tumor medium. Also, by comparing the drug release in the conditions (ii), better performance of the RMSN-DHPAN was observed. In general, RMSN-DHPAN had more sensitive behavior against temperature and pH changes. Therefore, using the hybrid method in modifying the surface of RMSN-D with plasma, has had a significant effect on increasing the drug delivery efficiency of mesoporous silica nanoparticles in the cancerous site.

Please cite this article as: S. Porrang et al., Direct surface modification of mesoporous silica nanoparticles by DBD plasma as a green approach to prepare dual-responsive drug delivery system, Journal of the Taiwan Institute of Chemical Engineers (2021), https://doi.org/10.1016/j.jtice.2021.05.024

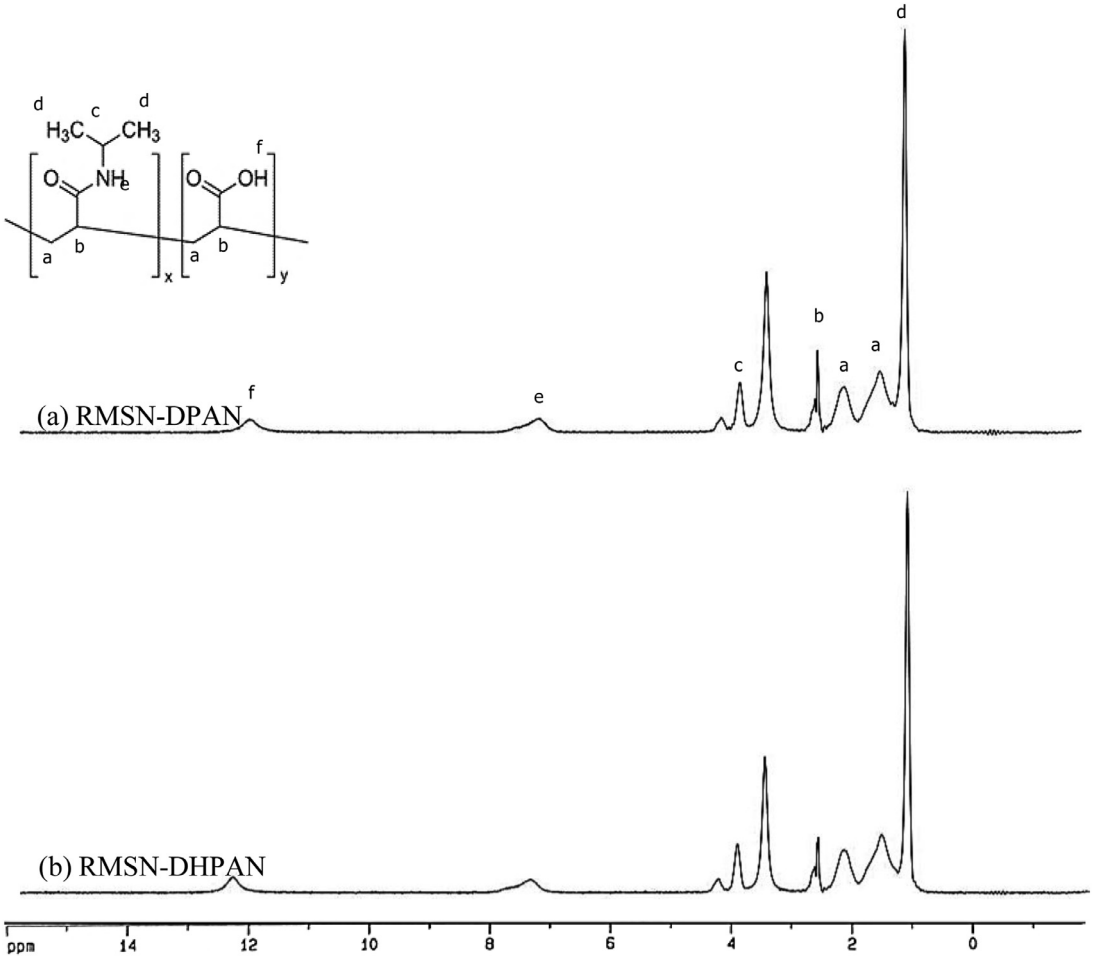

Fig. 5. ^{1}H NMR spectra of the (a) RMSN-DPAN, and (b) RMSN-DHPAN.

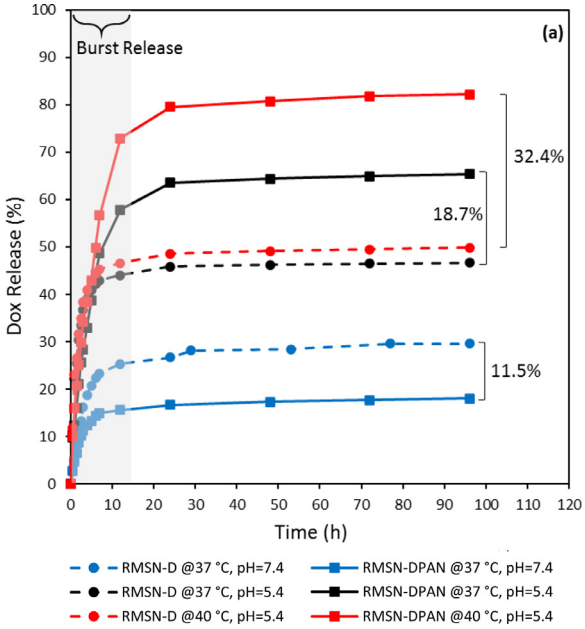

Fig. 6. Dox release profiles from (a) Dox-loaded RMSN-D, Dox-loaded RMSN-DPAN, (b) Dox-loaded RMSN-D, Dox-loaded RMSN-DHPAN, and (c) Comparison of the Dox-loaded RMSN-DPAN and Dox-loaded RMSN-DHPAN release during 4 days.

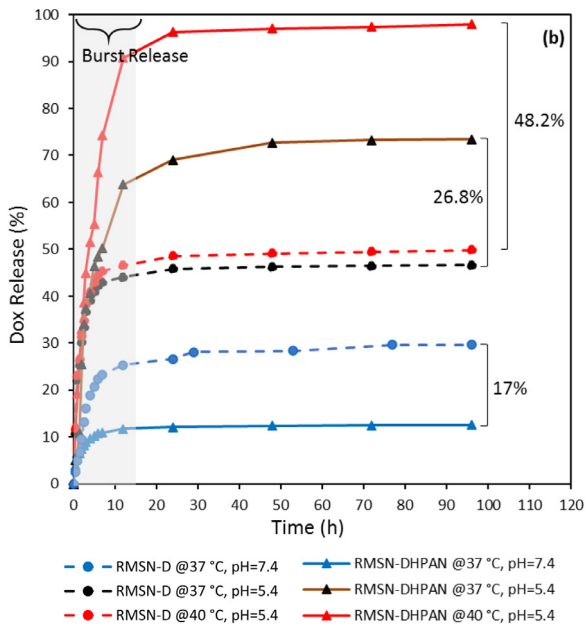

Fig. 6. Continued.

Please cite this article as: S. Porrang et al., Direct surface modification of mesoporous silica nanoparticles by DBD plasma as a green approach to prepare dual-responsive drug delivery system, Journal of the Taiwan Institute of Chemical Engineers (2021), https://doi.org/10.1016/j.jtice.2021.05.024

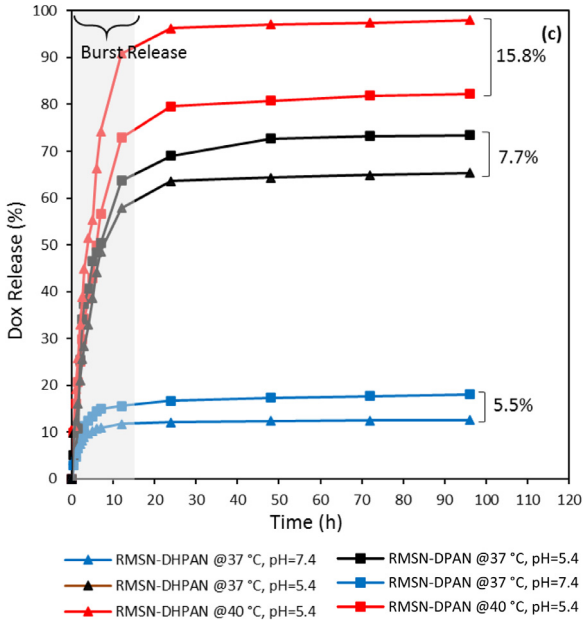

Fig. 6. Continued.

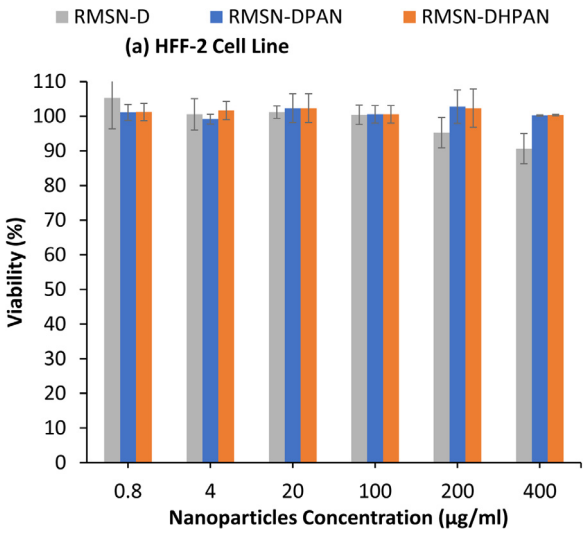

Fig. 7. The cytotoxicity and of different nanoparticles on (a) HFF-2 clells, (b) blank nanoparticles on MCF-7 cells and (c) Dox-loaded nanoparticles on MCF-7 cells.

4.4. MTT assay

The HFF-2 cell line as normal model cells were chosen for cytotoxicity and biocompatibility evaluation of nanocarriers. Depending on Fig. 7-a, 90% of the HFF-2 cells treated with RMSN-D were alive at a concentration of 400 μg mL^{-1} after 48 h. By modification and functionalization of the RMSN-D surface by biocompatible polymers, this amount had been increased to 100%. So, the functionalization improved the biocompatibility of nanocarriers. Overall, no significant toxicity of the nanocarriers was observed in the nanocarrier's concentration ranging from 0.8 to 400 μg mL^{-1}. Also, the potential of Dox-loaded nanocarriers was investigated by evaluating the cytotoxicity of samples on the MCF-7 cells with the Dox concentration ranging from 0.08 to 20 μg mL^{-1} during 48 h. As shown in Fig. 7-b, the blank nanocarriers showed no toxicity on MCF-7 cell line at the same Dox concentration after 48 h. However, as expected, by treating the cells with free Dox and Dox-loaded nanaocarriers, the dose-dependent inhibition of MCF-7 cell's proliferation was observed. As shown

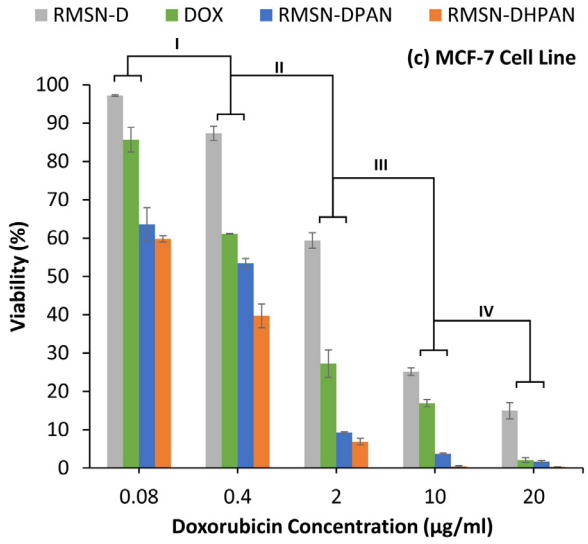

Fig. 7. Continued.

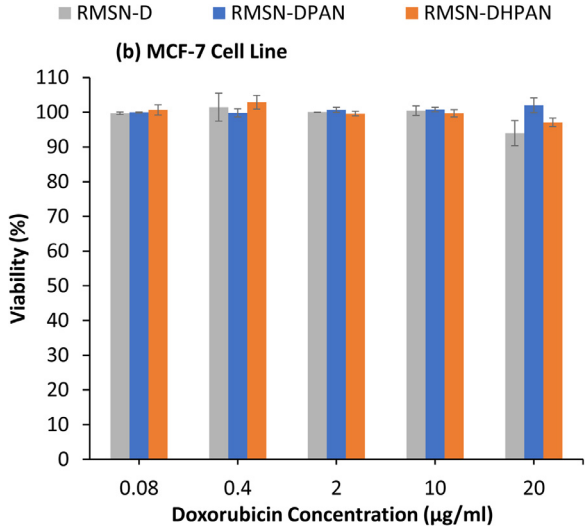

Fig. 7. Continued.

in Fig. 7-c, the Dox-loaded RMSN-D showed mild toxicity on MCF-7 cells compared with free Dox. However, the Dox-loaded RMSN-DPAN and Dox-loaded RMSND-HPAN had more toxic behavior against MCF-7 cells than Dox-loaded RMSN-D and free Dox. This toxicity enhancement can be explained by higher Dox releasing amount compared with Dox-loaded RMSN-D and sustained Dox released from them compared with free Dox. Moreover, it was clear that by hybrid plasma modification, the toxicity of RMSN-DHPAN enhanced compared with RMSN-DPAN due to higher Dox amount in the cancerous medium.

Enhanced toxicity of Dox-loaded RMSN-DPAN and especially Dox-loaded RMSN-DHPAN on cancerous cells compared to the free form of Dox would be advantage in reducing the anticancer dose and side effects in clinical cancer treatment applications. So, the hybrid plasma modification of mesoporous silica nanoparticles can act as a high-efficiency approach in drug delivery system designing and functionalization.

4.5. Cell cycle inhabitation

The cell cycle distribution pattern of untreated MCF-7 cells and treated MCF-7 cells with Dox-loaded nanocarriers was determined by the flow cytometry approach based on PI staining.

Please cite this article as: S. Porrang et al., Direct surface modification of mesoporous silica nanoparticles by DBD plasma as a green approach to prepare dual-responsive drug delivery system, Journal of the Taiwan Institute of Chemical Engineers (2021), https://doi.org/10.1016/j.jtice.2021.05.024

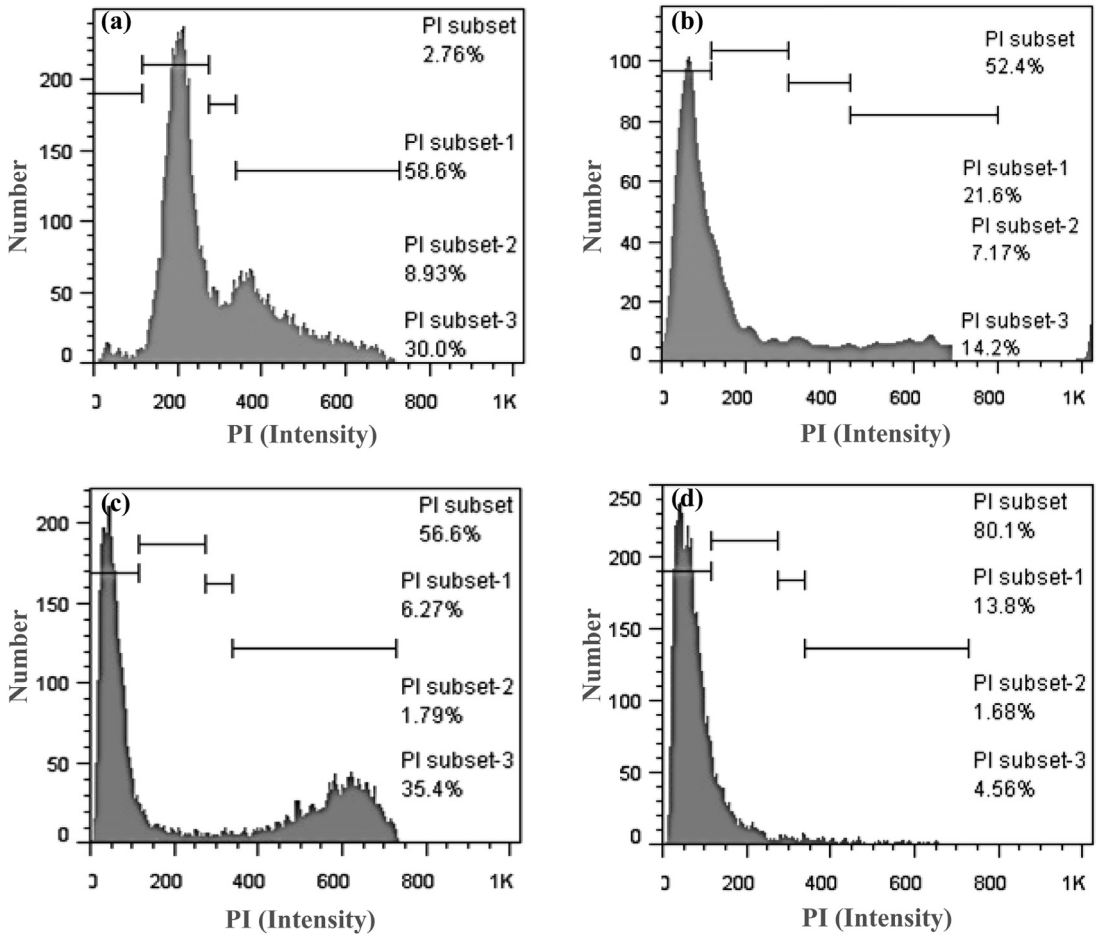

Fig. 8. Cell cycle analysis of the MCF-7 cells a) control, b) treated with Dox-loaded RMSN-D, c) Dox-loaded RMSN-DPAN, and Dox-loaded RMSN-DHPAN. The cells were treated with the IC50 value and harvested after 48 h.

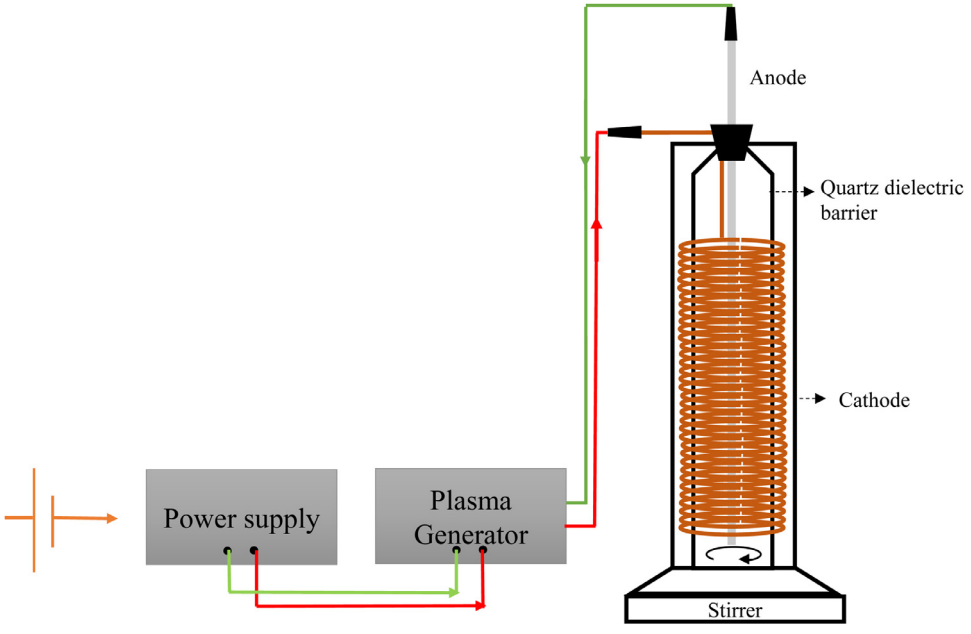

Scheme 1. The DBD plasma set up Consists of power supply, DC generator, DBD plasma, and stirrer.

Please cite this article as: S. Porrang et al., Direct surface modification of mesoporous silica nanoparticles by DBD plasma as a green approach to prepare dual-responsive drug delivery system, Journal of the Taiwan Institute of Chemical Engineers (2021), https://doi.org/10.1016/j.jtice.2021.05.024

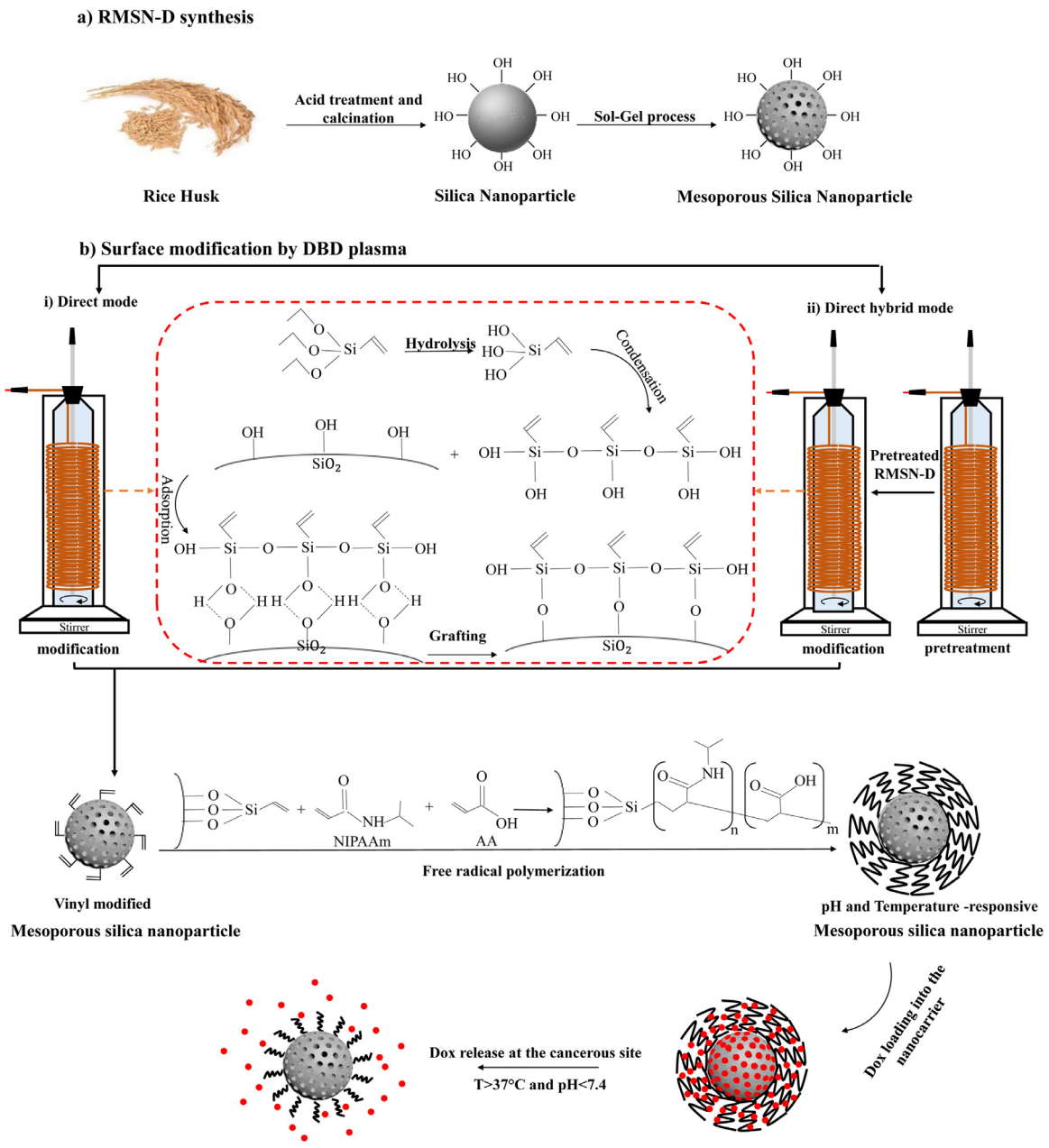

Scheme 2. The overall procedure of mesoporous silica nanoparticles synthesis from rice husk and b) nanoparticles surface modification synthesis by DBD plasma modification with i) Direct and ii) direct hybrid modes to pH and Temperature-responsive drug delivery system synthesis.

The cells were treated for 48 with an IC50 value of Dox-loaded RMSN-D, Dox-loaded RMSN-DPAN, and Dox loaded RMSN-DHPAN; Then, they were analyzed by flow cytometry. As shown in Fig. 8, the control MCF-7 cells were distributed among Sub-G1, G0/G1, S, and G2/M phases by almost 2.76%, 58.6%, 8.93%, and 30.0%, respectively. After incubation cells with Dox-loaded nanocarriers for 48 h, the percent of the Sub-G1 phase was increased to 52.40%, 56.6%, and 80.1%, respectively. The results showed that the Dox loaded nanoparticles, specially Dox@ RMSN-DHPAN, arrest the cell cycle in the Sub-G1 phase [35] and induced a high level of apoptosis in the MCF-7 cells.

4.6. Morphological assay of the apoptotic cells

For the morphological study of untreated MCF-7 cells and treated MCF-7 cells by Dox loaded nanocarriers and free Dox, the cells were stained with Hoechst 33,258 to detect the apoptotic cells. As shown in Fig. 9, under a fluorescence microscope, the untreated MCF-7 cell nucleus was large and round, without any condensation and fragmentation [44]. However, cells treated by Dox-loaded RMSN-D, Dox-loaded RMSN-DPAN, Dox loaded RMSN-DHPAN, and free Dox exhibited chromatin condensation and fragmentation, a typical morphological feature of apoptosis. As illustrated in Fig. 9, the chromatin condensation and fragmentation were more comprehensive (the apoptotic cells were represented by Arrows) in the cells were treated by Dox-loaded RMSN-DPAN, and especially RMSN-DHPAN. These results are in line with the previous observations, indicate the high capacity of RMSN-DHPAN in drug delivery and cancer treatment applications.

5. Conclusion

In the present work, an economic and biocompatible smart drug delivery system based on a natural source,which modified by DBD plasma was synthesized. The Biogenic mesoporous silica

Please cite this article as: S. Porrang et al., Direct surface modification of mesoporous silica nanoparticles by DBD plasma as a green approach to prepare dual-responsive drug delivery system, Journal of the Taiwan Institute of Chemical Engineers (2021), https://doi.org/10.1016/j.jtice.2021.05.024

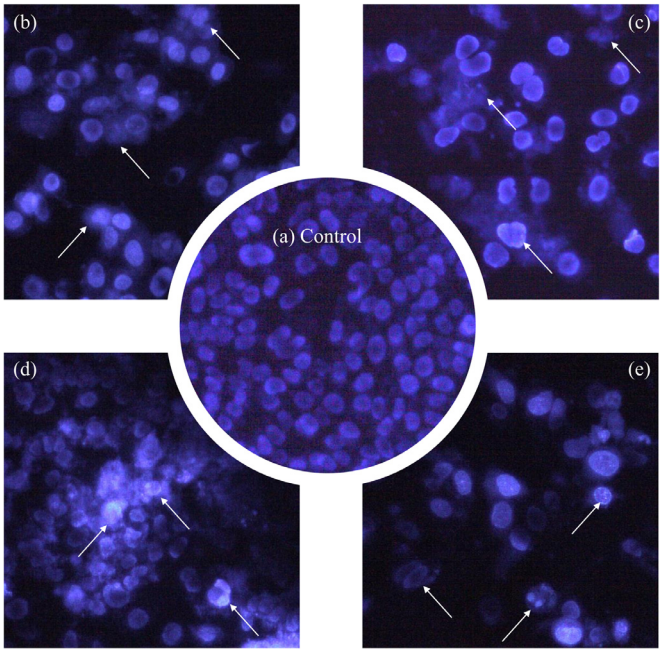

Fig. 9. Fluorescence microscopy of the MCF-7 cells treated with the a) control b) treated with Dox-loaded RMSN-D c) Dox-loaded RMSN-DPAN, d) Dox-loaded RMSN-DHPAN, and e) Dox. Fluorescence images of the cells stained with Hoechst 33,258 after 48 h. All the investigated chromenes induced condensation and fragmentation of the nuclei. Arrows represent apoptotic cells.

nanoparticles were uniformly modified by a DBD plasma in the direct, and the direct hybrid modes, and formed spherical nanoparticles of the same size. The PAA and PNIPAAm polymers were created on the surface of the modified nanoparticle to generated RMSN-DPAN and RMSN-DHPAN as stimuli-responsive drug delivery systems. The results demonstrate the higher stimuli-responsibility of RMSN-DHPAN against temperature and pH variation. Also, by biocompatibility evaluation of blank nanocarriers on the HFF-2, no significant toxicity was observed. Moreover, Dox-loaded RMSN-DPAN and especially Dox-loaded RMSN-DHPAN showed a higher cytotoxic effect on the MCF-7 cell line. As expected, advanced cellular tests also confirmed this result. So, The use of the DBD plasma system in surface modification had a significant effect on the drug delivery system's performance. In conclusion, RMSN-DPAN and especially RMSN-DHPAN had high potential application in temperature and pH-responsive controlled drug release and cancer treatment.

Declaration of Competing Interest

None.

Acknowledgments

The authors gratefully acknowledge Iran National Science Foundation for the financial support of the research under project number of 97014149 as well as Sahand University of Technology for complementary financial supports.

References

[1] Porrang S, Rahemi N, Davaran S, Mahdavi M, Hassanzadeh B. Synthesis of temperature/pH dual-responsive mesoporous silica nanoparticles by surface modification and radical polymerization for anti-cancer drug delivery. Colloid Surf A 2021:126719.
[2] Chen S, Xing C, Huang D, Zhou C, Ding B, Guo Z, et al. Eradication of tumor growth by delivering novel photothermal selenium-coated tellurium nanoheterojunctions. Sci Adv, 6; 2020. p. 2020eaay6825.
[3] Qiu M, Singh A, Wang D, Qu J, Swihart M, Zhang H, et al. Biocompatible and biodegradable inorganic nanostructures for nanomedicine: silicon and black phosphorus. Nano Today 2019;25:135–55.
[4] Hao N, Li L, Tang F. Roles of particle size, shape and surface chemistry of mesoporous silica nanomaterials on biological systems. Int Mater Rev 2017;62:57–77.
[5] Lv X, Zhang L, Xing F, Lin H. Controlled synthesis of monodispersed mesoporous silica nanoparticles: particle size tuning and formation mechanism investigation. Microporous Mesoporous Mater 2016;225:238–44.
[6] Tang F, Li L, Chen D. Mesoporous silica nanoparticles: synthesis, biocompatibility and drug delivery. Adv Mater 2012;24:1504–34.
[7] Porrang S, Rahemi N, Davaran S, Mahdavi M, Hassanzadeh B. Preparation and in-vitro evaluation of mesoporous biogenic silica nanoparticles obtained from rice and wheat husk as a biocompatible carrier for anti-cancer drug delivery. Eur J Pharm Sci 2021:105866.
[8] Elbialy NS, Aboushoushah SF, Sofi BF, Noorwali A. Multifunctional curcumin-loaded mesoporous silica nanoparticles for cancer chemoprevention and therapy. Microporous Mesoporous Mater 2020;291:109540.
[9] Guo Y, Wu L, Gou K, Wang Y, Hu B, Pang Y, et al. Functional mesoporous silica nanoparticles for delivering nimesulide with chiral recognition performance. Microporous Mesoporous Mater 2020;294:109862.
[10] Nik AB, Zare H, Razavi SS, Mohammadi H, Torab-Ahmadi P, Yazdani N, et al. Smart drug delivery: capping strategies for mesoporous silica nanoparticles. Microporous Mesoporous Mater 2020:110115.
[11] Díaz-García D, Sommerova L, Martisova A, Skoupilova H, Prashar S, Vaculovic T, et al. Mesoporous silica nanoparticles functionalized with a dialkoxide diorganotin (IV) compound: in search of more selective systems against cancer cells. Microporous Mesoporous Mater 2020:110154.
[12] Lim E-B, Vy TA, Lee S-W. Comparative release kinetics of small drugs (ibuprofen and acetaminophen) from multifunctional mesoporous silica nanoparticles. J Mater Chem B 2020;8:2096–106.
[13] Zaharudin NS, Isa EDM, Ahmad H, Rahman MBA, Jumbri K. Functionalized mesoporous silica nanoparticles templated by pyridinium ionic liquid for hydrophilic and hydrophobic drug release application. J Saudi Chem Soc 2020;24:289–302.
[14] Saini K, Prabhuraj R, Bandyopadhyaya R. Development of mesoporous silica nanoparticles of tunable pore diameter for superior gemcitabine drug delivery in pancreatic cancer cells. J Nanosci Nanotechnol 2020;20:3084–96.
[15] Costa JAS, de Jesus RA, Santos DO, Mano JF, Romão LP, Paranhos CM. Recent progresses in the adsorption of organic, inorganic, and gas compounds by MCM-41-based mesoporous materials. Microporous Mesoporous Mater 2020;291:109698.
[16] Isaeva V, Chernyshev V, Fomkin A, Shkolin A, Veselovsky V, Kapustin G, et al. Preparation of novel hybrid catalyst with an hierarchical micro-/mesoporous structure by direct growth of the HKUST-1 nanoparticles inside mesoporous silica matrix (MMS). Microporous Mesoporous Mater 2020:110136.
[17] Haynes T, Bougnouch O, Dubois V, Hermans S. Preparation of mesoporous silica nanocapsules with a high specific surface area by hard and soft dual templating approach: application to biomass valorization catalysis. Microporous Mesoporous Mater 2020:110400.
[18] Venezia V, Sannino F, Costantini A, Silvestri B, Cimino S, Califano V. Mesoporous silica nanoparticles for β-glucosidase immobilization by templating with a green material: tannic acid. Microporous Mesoporous Mater 2020:110203.
[19] Wang Y, Zhao Q, Han N, Bai L, Li J, Liu J, et al. Mesoporous silica nanoparticles in drug delivery and biomedical applications. Nanomed 2015;11:313–27.
[20] Hu X, Hao X, Wu Y, Zhang J, Zhang X, Wang PC, et al. Multifunctional hybrid silica nanoparticles for controlled doxorubicin loading and release with thermal and pH dual response. J Mater Chem B 2013;1:1109–18.
[21] Karabulut HRF, Mert B, Altinkok C, Karatavuk AO, Acik G, Turkyilmaz M. Synthesis of new bio-based hydrogels derived from bile acids by free-radical photo-polymerization. Polym Adv Technol 2021;32:220–7.
[22] Ojah N, Saikia D, Gogoi D, Baishya P, Ahmed GA, Ramteke A, et al. Surface modification of core-shell silk/PVA nanofibers by oxygen dielectric barrier discharge plasma: studies of physico-chemical properties and drug release behavior. Appl Surf Sci 2019;475:219–29.
[23] Ojah N, Deka J, Haloi S, Kandimalla R, Gogoi D, Medhi T, et al. Chitosan coated silk fibroin surface modified by atmospheric dielectric-barrier discharge (DBD) plasma: a mechanically robust drug release system. J Biomater Sci Polym Ed 2019;30:1142–60.
[24] Das P, Ojah N, Kandimalla R, Mohan K, Gogoi D, Dolui SK, et al. Surface modification of electrospun PVA/chitosan nanofibers by dielectric barrier discharge plasma at atmospheric pressure and studies of their mechanical properties and biocompatibility. Int J Biol Macromol 2018;114:1026–32.
[25] Ojah N, Borah R, Ahmed GA, Mandal M, Choudhury AJ. Surface modification of electrospun silk/AMOX/PVA nanofibers by dielectric barrier discharge plasma: physiochemical properties, drug delivery and in-vitro biocompatibility. Prog Biomater 2020;9:219–37.
[26] Taraballi F, Zanini S, Lupo C, Panseri S, Cunha C, Riccardi C, et al. Amino and carboxyl plasma functionalization of collagen films for tissue engineering applications. J Colloid Interface Sci 2013;394:590–7.
[27] Yan W, Phung B, Han Z, Ostrikov K. Plasma functionalization of SiO 2 nanoparticles for the synthesis of polymer nano-dielectrics. 2012 IEEE 10th International Conference on the Properties and Applications of Dielectric Materials. IEEE; 2012. p. 1–4.
[28] Rahemi N, Haghighi M, Babaluo AA, Allahyari S, Jafari MF. Syngas production from reforming of greenhouse gases CH4/CO2 over Ni–Cu/Al2O3 nanocatalyst: impregnated vs. plasma-treated catalyst. Energy Convers Manag 2014;84:50–9.

Please cite this article as: S. Porrang et al., Direct surface modification of mesoporous silica nanoparticles by DBD plasma as a green approach to prepare dual-responsive drug delivery system, Journal of the Taiwan Institute of Chemical Engineers (2021), https://doi.org/10.1016/j.jtice.2021.05.024

[29] Yuan M-H, Wang L, Yang RT. Glow discharge plasma-assisted template removal of SBA-15 at ambient temperature for high surface area, high silanol density, and enhanced CO2 adsorption capacity. Langmuir 2014;30:8124–30.
[30] Øye G, Roucoules V, Oates L, Cameron A, Cameron N, Steel P, et al. Plasmachemical amine functionalization of porous polystyrene spheres: the importance of particle size. J Phys Chem B 2003;107:3496–9.
[31] Chu PK, Chen J, Wang L, Huang N. Plasma-surface modification of biomaterials. Mater Sci Eng 2002;36:143–206.
[32] Laroussi M, Richardson JP, Dobbs FC. Effects of nonequilibrium atmospheric pressure plasmas on the heterotrophic pathways of bacteria and on their cell morphology. Appl Phys Lett 2002;81:772–4.
[33] Ferrari M. Cancer nanotechnology: opportunities and challenges. Nat Rev cancer 2005;5:161–71.
[34] Aryapour H, Mahdavi M, Mohebbi SR, Zali MR, Foroumadi A. Anti-proliferative and apoptotic effects of the derivatives from 4-aryl-4H-chromene family on human leukemia K562 cells. Arch Pharm Res 2012;35:1573–82.
[35] Mehdipour M, Dehghan G, Yekta R, Hanifeh Ahagh M, Mahdavi M, Ghasemi Z, et al. DNA-binding affinity, cytotoxicity, apoptosis, cell cycle inhibition and molecular docking studies of a new stilbene derivative. Nucleoside Nucleotide Nucleic Acid 2019;38:101–18.
[36] La-Salvia N, Lovón-Quintana JJ, Lovón ASP, Valença GP. Influence of aluminum addition in the framework of MCM-41 mesoporous molecular sieve synthesized by non-hydrothermal method in an alkali-free system. Mater Res 2017;20:1461–9.
[37] Nam I, Bae JW, Jee KS, Lee JW, Park KD, Yuk SH. Poly (N-isopropylacrylamide-co-N-vinylpyrrolidone) as a novel implant materials: preparation and thermo-gelling behavior. Macromol Res 2002;10:115–21.
[38] Jin S, Liu M, Chen S, Gao C. Synthesis, characterization and the rapid response property of the temperature responsive PVP-g-PNIPAM hydrogel. Eur Polym J 2008;44:2162–70.
[39] Salehi R, Hamishehkar H, Eskandani M, Mahkam M, Davaran S. Development of dual responsive nanocomposite for simultaneous delivery of anticancer drugs. J Drug Target 2014;22:327–42.
[40] Gao X, Cao Y, Song X, Zhang Z, Xiao C, He C, et al. pH-and thermo-responsive poly (N-isopropylacrylamide-co-acrylic acid derivative) copolymers and hydrogels with LCST dependent on pH and alkyl side groups. J Mater Chem B 2013;1:5578–87.
[41] Knežević, N.Ž., .Trewyn, B.G., Lin, V.S.Y., "Light-and pH-responsive release of doxorubicin from a mesoporous silica-based nanocarrier". Chemistry, 17: pp. 3338–42, (2011).
[42] Karanth H, Murthy R. pH-Sensitive liposomes-principle and application in cancer therapy. J Pharm Pharmacol 2007;59:469–83.
[43] Hu X, Wei W, Qi X, Yu H, Feng L, Li J, et al. Preparation and characterization of a novel pH-sensitive Salecan-g-poly (acrylic acid) hydrogel for controlled release of doxorubicin. J Mater Chem B 2015;3:2685–97.
[44] Naseri MH, Mahdavi M, Davoodi J, Tackallou SH, Goudarzvand M, Neishabouri SH. Up regulation of Bax and down regulation of Bcl2 during 3-NC mediated apoptosis in human cancer cells. Cancer Cell Int. 2015;15:55.

Please cite this article as: S. Porrang et al., Direct surface modification of mesoporous silica nanoparticles by DBD plasma as a green approach to prepare dual-responsive drug delivery system, Journal of the Taiwan Institute of Chemical Engineers (2021), https://doi.org/10.1016/j.jtice.2021.05.024